

First-principles calculations of current-induced spin-transfer torques in magnetic domain walls

Ling Tang, Zhijun Xu and Zejin Yang

Department of Applied Physics, Zhejiang University of Technology, Hangzhou 310023, P. R. China

Current-induced spin-transfer torques (STTs) have been studied in Fe, Co and Ni domain walls (DWs) by the method based on the first-principles noncollinear calculations of scattering wave functions expanded in the tight-binding linearized muffin-tin orbital (TB-LMTO) basis. The results show that the out-of-plane component of nonadiabatic STT in Fe DW has localized form, which is in contrast to the typical nonlocal oscillating nonadiabatic torques obtained in Co and Ni DWs. Meanwhile, the degree of nonadiabaticity in STT is also much greater for Fe DW. Further, our results demonstrate that compared to the well-known first-order nonadiabatic STT, the torque in the third-order spatial derivative of local spin can better describe the distribution of localized nonadiabatic STT in Fe DW. The dynamics of local spin driven by this third-order torques in Fe DW have been investigated by the Landau-Lifshitz-Gilbert (LLG) equation. The calculated results show that with the same amplitude of STTs the DW velocity induced by this third-order term is about half of the wall speed for the case of the first-order nonadiabatic STT.

PACS numbers:

I. INTRODUCTION

The dynamics of the magnetic domain wall (DW) driven by electric current-induced spin-transfer torque (STT) is under extensive both experimental¹⁻⁹ and theoretical¹⁰⁻¹⁶ investigations in recent years. As known to all, in general the DW motion can be driven by an external magnetic field¹⁷ and/or spin-polarized electric current.^{18,19} For the magnetic field-driven case, although the well-known Walker's theory¹⁷ is usually used to understand the phenomena of DW movement induced by magnetic field, the origin of this motion is beyond the scope of Walker's theory. However, X. R. Wang *et al.*^{20,21} recently found that the mechanism of DW propagation by external magnetic field in a nanowire can attribute to the energy dissipation that is owing to Gilbert damping. On the other hand for the current-induced case, when an electron passes through a magnetic DW, it will be scattered by the noncollinear magnetic structure, which results in the phenomenon of magnetoresistance (MR).²² Meanwhile, the conduction electron can also transfer the spin angular momentum to the local spin when it flows through the DW. So a spin-transfer torque will exert on the local magnetic moment and then the electric current can be used to manipulate the magnetic structure of DW. This phenomenon of STT including current-induced DW motion was first predicted and observed in the experiments by L. Berger and coworkers.²³⁻²⁵ Moreover, this exotic phenomenon will also have some potential applications such as magnetic random-access memories (MRAMS),^{26,27} racetrack memories,^{28,29} spin transfer nano oscillators (STNOs)^{19,30,31} etc., which have attracted a great deal of attention recently.

For a DW in the adiabatic approximation, the spin of the incident electrons can be consistently aligned with the local spin moments. The spatial derivative of this adiabatic spin current yields the adiabatic STT which is written as $-b_J \partial_y \mathbf{S}$, where \mathbf{S} is the local spin of DW

and y is coordinate in transport direction.³²⁻³⁴ Here b_J is parameter with unit [m/s] in proportion to current density. However, there are always some conduction electron spins that cannot follow the local spin moments as the width of DW decreasing. The process that the spin of conduction electron relax toward the local spin moments will cause a nonadiabatic torque³⁵⁻³⁷ called the β term, which is in the form of $-\beta b_J \mathbf{n} \times \partial_y \mathbf{S}$, where β is the dimensionless parameter and $\mathbf{n} = \mathbf{S}/|\mathbf{S}|$ is the unit vector of local spin moments. Further, S. Zhang and Z. Li³⁵ have pointed out that the adiabatic STT only contributes the initial velocity of DW movement while the nonadiabatic term mentioned above determines the terminal velocity observed in experiments.

However, for the relative narrow DW a nonlocal oscillating torques have been predicted theoretically by several groups^{36,38,39} and its quantum origin is similar to the RKKY oscillation.¹³ Moreover, in general the ratio between the maximum of nonadiabatic and adiabatic STT, such as the coefficient β mentioned above, represents the degree of nonadiabaticity which can determine the velocity of DW movement.³⁵ So one of the purposes in this paper is to find out whether there is a nonlocal oscillating or localized torques in real ferromagnetic materials by calculating the STT of DW using the first-principles method. And the other purpose is to study the difference in magnitude of nonadiabatic STT among the traditional ferromagnetic DWs (Fe, Co and Ni).

On the other hand, M. Thorwart and R. Egger⁴⁰ have derived a torque in form of the second-order spatial derivative of the local spin by a gradient expansion scheme. Hence, it is tempted to introduce a higher-order of nonadiabatic STT such as $\mathbf{n} \times \partial_y^3 \mathbf{S}$ into the current-induced DW dynamics.⁴¹ So in this paper we will figure out whether there is higher-order torque in DW for real ferromagnetic materials. In addition, the effect of such higher-order STT on the DW movement is also needed for better understanding of current-induced DW dynam-

ics.

In this paper, we will study the current-induced STT of defect-free DW in ballistic limit by the first-principles electronic structure calculations.^{42–44} Our results show that the nonadiabatic STT of Fe DW has localized form while the out-of-plane STTs of Co and Ni are typical non-local oscillating torques. The degree of nonadiabaticity is also much greater for Fe DW and increases exponentially with decreasing the width of DW. In addition, the results also show that the distribution of our calculated nonadiabatic STT for Fe DW can well describe by the third-order spatial derivative term as $\mathbf{n} \times \partial_y^3 \mathbf{S}$. Finally, the dynamics of local spin in DW pushed by this third-order STT is simulated using Landau-Lifshitz-Gilbert (LLG) equation. The obtained time evolution of DW movement demonstrates that with the same amplitude of the nonadiabatic STT the velocity owing to the third-order STT will be reduced to about half of the wall speed induced by the first-order term.

II. METHOD

Our calculation of STT for DW is based on the scattering wave function matching (WFM) method with tight-binding linear muffine-tin orbital (TB-LMTO) basis.^{42,45} For a typical Néel or Bloch DW, the left and right domains act as leads and the wall structure is regarded as the scattering region, which defines the completed scattering problem of layered system as shown in Fig. 1. For this layered system, we assumed that the magnetization of DW has lattice translation invariant in the plane perpendicular to transport direction, so the operator and scattering states can be characterized by a lateral \mathbf{k}_{\parallel} wave vector in two-dimension (2D) Brillouin zone (BZ).

In this paper, the STT is calculated from the spin current, which is defined as

$$\hat{\mathcal{J}} \equiv \frac{1}{2} [\hat{\sigma} \otimes \hat{\mathbf{V}} + \hat{\mathbf{V}} \otimes \hat{\sigma}]. \quad (1)$$

where $\hat{\sigma}$ is Pauli spin matrix and $\hat{\mathbf{V}}$ is velocity operator. In the mixed representation for a special \mathbf{k}_{\parallel} with real space quasi one-dimension (1D) tight-binding model, the spin current operator from \mathbf{R}' th to \mathbf{R} th site is⁴²

$$\hat{\mathcal{J}}_{\mathbf{R}',\mathbf{R}}(\mathbf{k}_{\parallel}) = \sum_{LL'} \frac{1}{2i\hbar} [\hat{\sigma} \hat{\mathbf{H}}_{\mathbf{R}L,\mathbf{R}'L'}^{\mathbf{k}_{\parallel}} + \hat{\mathbf{H}}_{\mathbf{R}L,\mathbf{R}'L'}^{\mathbf{k}_{\parallel}} \hat{\sigma} - h.c.]. \quad (2)$$

where $\hat{\mathbf{H}}_{\mathbf{R}L,\mathbf{R}'L'}^{\mathbf{k}_{\parallel}}$ is noncollinear TB-LMTO Hamiltonian matrix element in the global quantum axis representation. Here $L \equiv (l, m)$, where l and m are the azimuthal and magnetic quantum numbers respectively.

In order to obtain $\hat{\mathbf{H}}_{\mathbf{R}L,\mathbf{R}'L'}^{\mathbf{k}_{\parallel}}$ of DW, firstly the collinear Hamiltonian from self-consistent one-electron effective potential of the magnetic materials is calculated by collinear electronic structure calculation in atom sphere approximation (ASA).^{46–48} Next, by introducing the

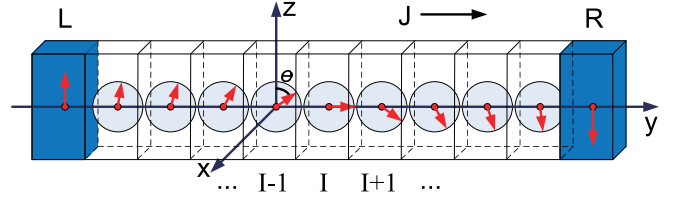


FIG. 1: Sketch of the completed scattering problem of layered system for Néel-type domain wall. The red arrows distributed in y - z plane denote the local spin moments whose polar angle is θ . Note that the current (J) flows from the left (L) lead to the right (R) lead and I is layer index.

rigid potential approximation,^{42,43,49} we rotate the above Hamiltonian, which is diagonal in 2×2 spin space at local quantum axis representation, by unity rotation matrix $\hat{U}(\theta, \phi)$ in spin space to construct the noncollinear Hamiltonian in the global quantum axis representation. Here the rotation angle θ is determined by the local spin moments configuration of DW, which is written as

$$\theta(y_{\mathbf{R}}) = \frac{\pi}{2} + \arcsin[\tanh(\frac{y_{\mathbf{R}}}{\lambda_{\text{DW}}})] \quad (3)$$

where λ_{DW} is the characteristic length for DW and $\theta(y_{\mathbf{R}})$ is the polar angle of local spin on the \mathbf{R} th site with position $y_{\mathbf{R}}$ along transport direction. Here, the injected current is along fcc(111) direction for Co and Ni DW and bcc(001) direction for Fe DW. In our calculation, we choose the azimuthal angle $\phi(y_{\mathbf{R}}) = \pi/2$ for modeling Néel-type DW as shown in Fig. 1.

Using the WFM method, we can obtain the scattering wave function corresponding to the noncollinear Hamiltonian of DW. Therefore, for scattering state with lateral wave vector \mathbf{k}_{\parallel} , the expectation value of STT acting on local spin can be determined by the difference between the incoming and outgoing spin current on \mathbf{R} th site, i.e.,^{42,43}

$$\langle \hat{\mathbf{T}}_{\mathbf{R}}^s(\mathbf{k}_{\parallel}) \rangle = \sum_{\mathbf{R}' \in I-1, I} \langle \hat{\mathcal{J}}_{\mathbf{R}',\mathbf{R}}^s(\mathbf{k}_{\parallel}) \rangle - \sum_{\mathbf{R}' \in I, I+1} \langle \hat{\mathcal{J}}_{\mathbf{R},\mathbf{R}'}^s(\mathbf{k}_{\parallel}) \rangle. \quad (4)$$

where I is the index of principal layer in quasi-1D model and the \mathbf{R} th site belongs to the layer I . Here the superscript $s = \uparrow, \downarrow$ denotes that the scattering state for evaluating expectation value is induced by the injected electron in spin s with respect to the local quantum axis of lead. Then in the linear response regime, the total torque under a small bias V_b is calculated by summing all the STT of \mathbf{k}_{\parallel} states in 2D BZ, which can be written as^{42,43}

$$\mathbf{T}_{\mathbf{R}}(V_b) = \left(\frac{\hbar}{2} \right) \frac{e V_b}{2\hbar N_{\parallel}} \sum_{s, \mathbf{k}_{\parallel}} \left[\langle \hat{\mathbf{T}}_{\mathbf{R}}^s(\mathbf{k}_{\parallel}) \rangle_{\mathcal{L}} - \langle \hat{\mathbf{T}}_{\mathbf{R}}^s(\mathbf{k}_{\parallel}) \rangle_{\mathcal{R}} \right], \quad (5)$$

where N_{\parallel} is the number of \mathbf{k}_{\parallel} states in 2D BZ at Fermi level. Here \mathcal{L} and \mathcal{R} denote the STT induced by the left and right incoming electrons from the lead region

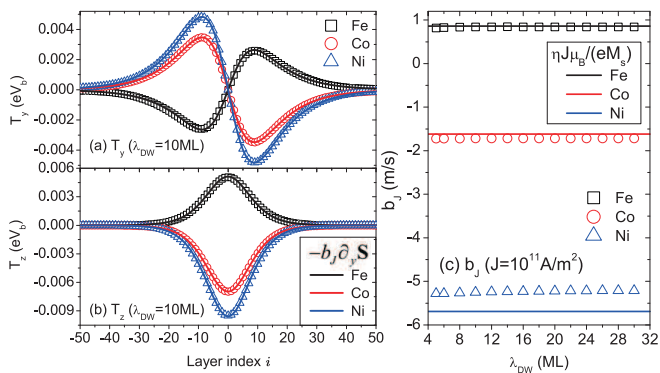


FIG. 2: The in-plane STT for Fe, Co and Ni DWs with $\lambda_{\text{DW}} = 10[\text{ML}]$ at unit bias. (a) y component of STT. (b) z component of STT. The solid line denote the fitting adiabatic STT in form of $-b_J \partial_y \mathbf{S}$. It can be seen that our calculated in-plane STTs agree well with the term of $-b_J \partial_y \mathbf{S}$. (c) The fitting results of b_J for different DW width at current density $J = 10^{11}[\text{A}/\text{m}^2]$. Here the solid line denote the predicted values of $b_J = \eta J \mu_B / (e M_s)$.

TABLE I: The parameter b_J at current density $J = 10^{11}[\text{A}/\text{m}^2]$ for $\lambda_{\text{DW}} = 10[\text{ML}]$, where η is the calculated polarization $\eta \equiv (G_{\uparrow} - G_{\downarrow}) / (G_{\uparrow} + G_{\downarrow})$, where $G_{\uparrow(\downarrow)}$ is sharvin conductance of leads for spin up (down) channel at Fermi level in our transport calculation. One can see that the values of our fitting b_J are close to $\eta J \mu_B / (e M_s)$.

DW	$G_{\uparrow} [\frac{\text{S}}{\text{m}^2}]$	$G_{\downarrow} [\frac{\text{S}}{\text{m}^2}]$	η	$M_s [\frac{\text{A}}{\text{m}}]$	$\frac{\eta J \mu_B}{e M_s} [\frac{\text{m}}{\text{s}}]$	$b_J [\frac{\text{m}}{\text{s}}]$
Fe	7.78×10^{14}	4.6×10^{14}	0.257	17.18×10^5	0.866	0.84
Co	4.59×10^{14}	10.8×10^{14}	-0.40	14.46×10^5	-1.60	-1.72
Ni	4.69×10^{14}	13.4×10^{14}	-0.48	4.9×10^5	-5.67	-5.25

respectively. In our calculations, the STTs of DW are performed with a $480 \times 480 \mathbf{k}_{\parallel}$ -mesh points in the lateral 2D BZ, which can insure convergence of the results.

III. RESULTS AND DISCUSSION

In this paper, we will investigate the nonadiabatic STT and corresponding dynamics of DW movement for the typical ferromagnetic materials Fe, Co and Ni. Firstly, Fig. 2(a) and (b) show the y and z component of STT for DW width $\lambda_{\text{DW}} = 10[\text{ML}]$. According to the configuration of Néel DW in Fig. 1, here the y and z component of torque is so-called in-plane STT and the x component is the out-of-plane STT. It can be seen that all these in-plane torques including Fe, Co and Ni agree well with the prediction of adiabatic approximation,³²⁻³⁴ which has the form of $-b_J \partial_y \mathbf{S}$. It is noted that the STT shown in Fig. 2(a) and (b) is at unit bias and the coefficient b_J is proportional to the current density. So combined with the corresponding ballistic conductance $G[\text{S}/\text{m}^2]$ of DW, we can use formula $-b_J \partial_y \mathbf{S}$ to fit the in-plane STT and obtain the coefficient b_J at unit current density. Here

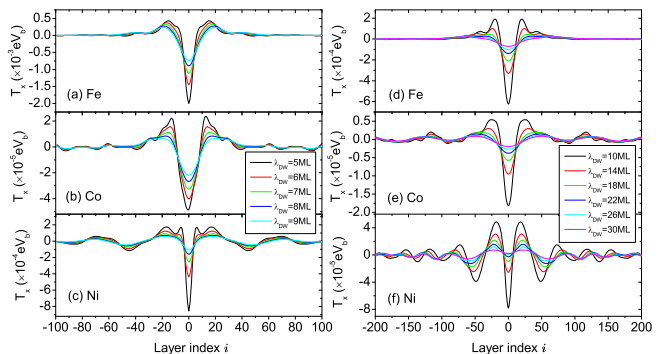


FIG. 3: The out-of-plane component of STTs for Fe, Co and Ni DWs with different λ_{DW} . One can observe that the out-of-plane STT of Fe DW has localized form while the spatial distribution of STTs for Co and Ni DW is nonlocal oscillating.

Table. 1 shows the fitting results of parameter b_J at current density $J = 10^{11}[\text{A}/\text{m}^2]$ for $\lambda_{\text{DW}} = 10[\text{ML}]$. One can observe that our fitting coefficients b_J for Fe, Co and Ni DWs are close to the values of $\eta J \mu_B / (e M_s)$, which is the prediction of the semiclassical transport theory,^{33,34} where η is the spin polarization of current, J is current density and M_s is saturated magnetization of ferromagnet. Here note that we use the calculated polarization $\eta \equiv (G_{\uparrow} - G_{\downarrow}) / (G_{\uparrow} + G_{\downarrow})$, where $G_{\uparrow(\downarrow)}$ is sharvin conductance of leads for spin up (down) channel at Fermi level in our transport calculation, instead of the values extracted from the experiments. The fitting results of b_J for different DW width are also shown in Fig. 2(c). It can be seen that the b_J is almost independent on DW width even for the narrow wall with $\lambda_{\text{DW}} = 5[\text{ML}]$.

Next, we will concentrate on the obtained out-of-plane nonadiabatic STT which is beyond the above in-plane adiabatic STT. Fig. 3 shows the spatial distribution of out-of-plane STT for different width λ_{DW} in Fe, Co and Ni DWs. One can observe that for Co and Ni DWs in the region far away from the DW center, where the magnetization is uniform, there is nonlocal oscillation in the distribution of out-of-plane torque. This nonlocal oscillating torques have already been discovered by several groups^{36,38,39} and G. Tataru *et al.*¹³ pointed out that the oscillating torques can be summed up as a collective force on the DW. In our calculations, this oscillating out-of-plane STT is contributed by the propagating states which precess around the local spin moments and has the form of $e^{i(k^{\uparrow} - k^{\downarrow})y}$, where $k^{\uparrow(\downarrow)}$ is wave vector in transport direction of propagating state.⁵⁰ Considering that the summation of propagating states over the 2D BZ in the transport calculation, the cancellation effect⁵⁰ in the different \mathbf{k}_{\parallel} make the oscillating behavior of out-of-plane torque depend on the shape of Fermi surface. Therefore, as shown in Fig. 3 the amplitude and diffusion length of torque oscillation is significant larger for Ni DW than that for Co DW, which is similar to the case of layered spin valve system.⁴² For the same reason as above, in Fig. 3(a) and (d) one can see that our cal-

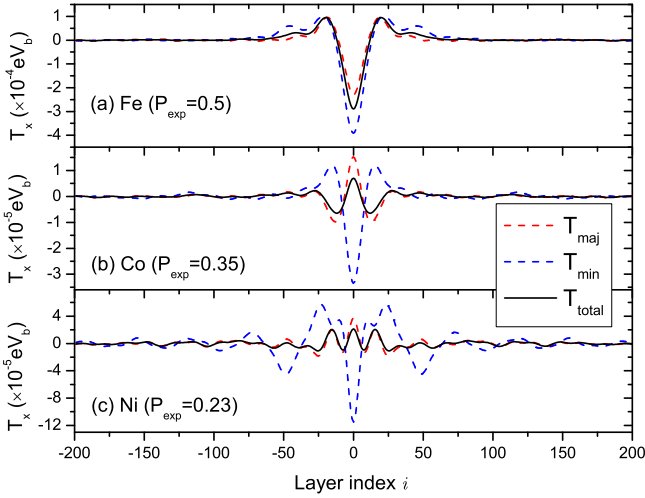


FIG. 4: The calculated distribution of out-of-plane STTs for DWs with $\lambda_{\text{DW}} = 10[\text{ML}]$ in the experimental current spin polarization. The black solid line denotes the total weighted STT, while the red and blue dash lines denote the STT induced only by incoming majority and minority electron respectively.

culated out-of-plane STT of Fe DW has localized form without oscillation far away from DW center except a small oscillation near the center region.

In our ballistic calculations, the spin polarization of the current is different with the experimental one. So in order to simulate the case of STT in experiments, firstly using the Eq. 5 we can obtain the STT induced only by the incoming majority (\mathbf{T}_{\uparrow}) and minority (\mathbf{T}_{\downarrow}) electron respectively. Then the total STT can be calculated by $\mathbf{T}_{\text{total}} = W_{\uparrow}\mathbf{T}_{\uparrow} + W_{\downarrow}\mathbf{T}_{\downarrow}$, where the weighting factors $W_{\uparrow(\downarrow)}$ is determined by $(W_{\uparrow}G_{\uparrow} - W_{\downarrow}G_{\downarrow})/(W_{\uparrow}G_{\uparrow} + W_{\downarrow}G_{\downarrow}) = P_{\text{exp}}$. Here P_{exp} is the experimental current spin polarization. Fig. 4 shows the distribution of the out-of-plane STTs for DWs with the experimental current spin polarization. One can observe that the results do not qualitatively change at all compared to the ballistic calculations, namely the out-of-plane STT of Co and Ni DWs have nonlocal oscillating forms while that of Fe DW has the localized form.

For the out-of-plane torque in the form of $-\beta b_j \mathbf{n} \times \partial_y \mathbf{S}$, it is believed that the coefficient β , which is just the ratio between the maximum of out-of-plane and in-plane STT, determine the final velocity v of DW motion by the expression³⁵ of $v = b_j \beta / \alpha$. And coefficient β is usually viewed as the degree of nonadiabaticity in STT. However, the form of out-of-plane nonadiabatic STT in our results is not exactly the same with the β term, but we still calculated the ratio between the out-of-plane and in-plane STT at the center of DW to demonstrate the degree of nonadiabaticity for DW with different materials. As shown in Fig. 5, one can see that with decreasing the DW width the nonadiabaticity will increase exponentially, which agree well with the calculation of

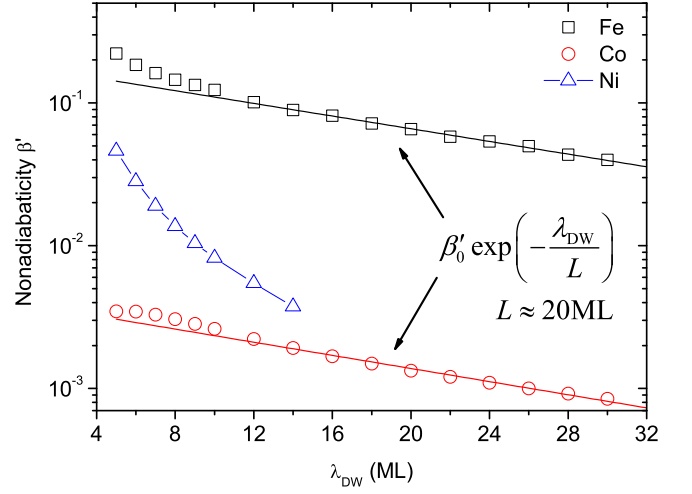


FIG. 5: The width dependence of nonadiabaticity for Fe, Co and Ni DWs. The nonadiabaticity β' is defined as the ratio between the out-of-plane and in-plane STT at DW center, namely $\beta' \equiv |T_x / \sqrt{T_y^2 + T_z^2}|_{y=0}$. It is noted that for Ni DW with $\lambda_{\text{DW}} > 14[\text{ML}]$ the oscillation of out-of-plane STT is so larger that the maximum is no longer at the center of DW. For $\lambda_{\text{DW}} > 10[\text{ML}]$ the nonadiabaticity of Fe and Co can be well fitted by $\beta' = \beta'_0 \exp(-\lambda_{\text{DW}}/L)$, where $L \approx 20[\text{ML}]$.

free-electron Stoner model.³⁸ Further, the nonadiabaticity for Co and Fe DWs have the same growth rate with decreasing λ_{DW} . Moreover, one can also observe that the nonadiabaticity of Fe DW is about one order larger than that of Co and Ni DWs. In the meantime, the value of nonadiabaticity for Fe DW even can be reach at a very high value (~ 0.2) for the narrow width $\lambda_{\text{DW}} = 5[\text{ML}]$. In general, there are two contributions to the nonadiabatic STT in DW. One is the spin relaxation process of the conducting electron spin toward local spin, the other is the mistracking between the incoming conducting electron spin and local spin without any relaxation. In our calculations, it is noted that there is no any dynamical relaxation process taken into account, thus only the mistracking contribution exists, which is similar to the case of free-electron Stoner model.³⁸ From Fig. 5, one can see that this mistracking contributed STTs for Co and Ni are too small to be measured in experiments with reasonable DW width. Therefore, it implied that the relaxation contributed nonadiabatic STT dominates in Co and Ni DWs.

Fig. 6 shows the comparison between the calculated out-of-plane STT and the torque of spatial derivative of the local spin. Here the torques in first- and third-order derivative are both depicted and their maximums are fitted to the calculated STT at center. At first glance, one can see that the configuration of the β term is much different with the calculated results from Fig. 6. In particular, the width of STT peak for β term at the DW center is much larger than that of the calculated STT. Hence, it suggested that this deviation may have a significant effect on the velocity of DW movement. However,

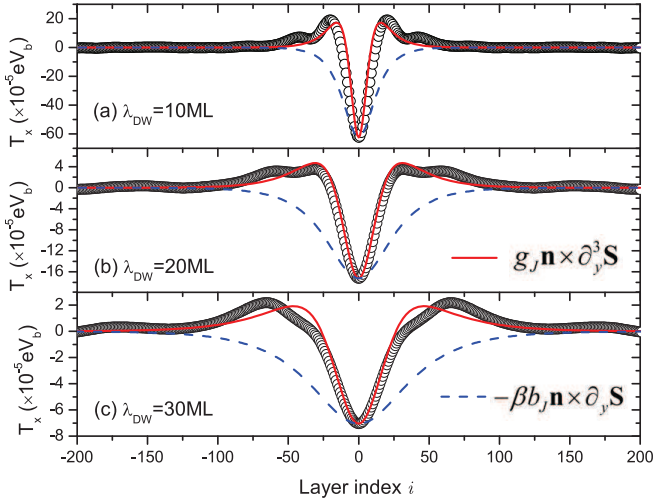


FIG. 6: The calculated distribution of out-of-plane STT and the spatial derivative of the local spin for Fe DW. Here the hollow circles are obtained STTs from the first-principles calculations. The blue dash line and red solid line denote the fitting results of β term and the torques in the third-order of the spatial derivative respectively. It shows that the term of $g_J \mathbf{n} \times \partial_y^3 \mathbf{S}$ can well describe the calculated out-of-plane STT of Fe DW.

the study of the DW movement using the first-principles calculated STT directly will cost too much computing time so that we can hardly obtain the results for a long time intervals. So in order to investigate the time evolution of DW more efficiently, here we will model a simple analytical nonadiabatic STT term substituted into the equations of DW dynamical evolution. As shown in Fig. 6, we found that compared to the β term, the nonadiabatic STT in the form of $g_J \mathbf{n} \times \partial_y^3 \mathbf{S}$, which is proportional to the third-order spatial derivative of the local spin, can well describe the obtained out-of-plane STT in Fe DW. Here g_J is the parameter in proportion to current density. The origin of this nonadiabatic STT may be similar with the β term. According to the gradient expansion scheme for STT⁴⁰, the first-order expansion will result in both adiabatic STT and nonadiabatic β term. Meanwhile, the higher-order expansion will lead to the second-order STT.⁴⁰ Therefore, based on the gradient expansion scheme, it is reasonable to obtain the torques in the third-order spatial derivative in our calculations.

On the other hand, at two sides of Fe DW center region there is still small difference between the calculated and the third-order STT, where the calculated STT also has small oscillating form. It implied that the reason of our calculated STT in Fe DW being well fitted by the third-order term maybe is due to the dephasing effect, where the oscillating STT can be canceled each other by summing the \mathbf{k}_{\parallel} states at Fermi surface. For Co and Ni DW the majority Fermi surface is similar to that of free-electron thus the dephasing effect is very weak, which makes the nonadiabatic STT still has oscillating form³⁸ as shown in Fig. 4(b) and (c). However, the Fermi

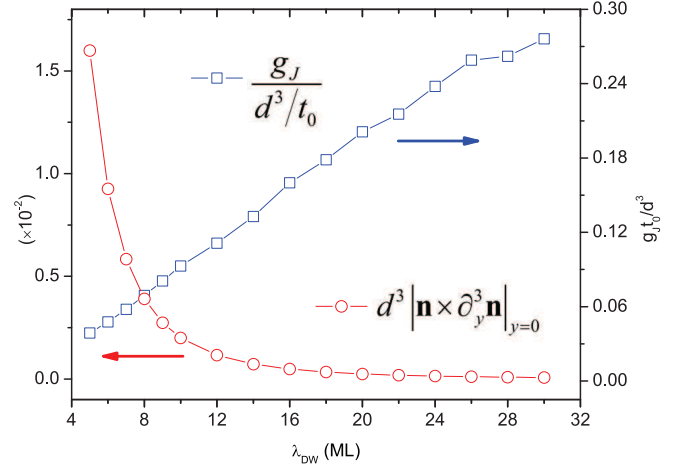


FIG. 7: The fitting results of dimensionless coefficient $g_J t_0 / d^3$ for Fe DW with different width at current density $J = 10^{11} [\text{A}/\text{m}^2]$, where d is the distance between the monolayers and the unit time is $t_0 = (4\pi M_s \gamma)^{-1}$. The dependence of spatial derivative at DW center ($y = 0$) on width λ_{DW} is also depicted in this figure. It can be seen that although g_J grows linearly with increasing λ_{DW} , the amplitude of the third-order torque still decays due to the term of $\mathbf{n} \times \partial_y^3 \mathbf{n}$.

surface of Fe is far beyond the free-electron-like one so the dephasing effect is much stronger in Fe DW. Meanwhile, the dephasing effect is not effective near the DW center and increases its effectiveness relatively rapidly with increasing distance from the DW center. Therefore, the corresponding nonadiabatic STT has the form of the third-order term. In particular, when the distance from DW center is not very large, the dephasing has not taken fully effect in such regions, so the oscillating behavior of STT will still emerge as shown in Fig. 6. Nevertheless, due to the dynamics of DW is mainly attribute to the STT in DW center, which is well fitted by the third-order STT as shown in Fig. 6, in this paper we will focus on how the nonadiabatic STT term in the form of $g_J \mathbf{n} \times \partial_y^3 \mathbf{S}$ will influence the velocity of DW movement.

For Fe DW with different width λ_{DW} at current density $J = 10^{11} [\text{A}/\text{m}^2]$, the fitting results of dimensionless coefficient $g_J t_0 / d^3$ is shown in Fig. 7, where g_J is in unit of $[\text{m}^3/\text{s}]$, $d = 1.43 \text{ \AA}$ is the distance between the monolayers and the unit time is $t_0 = (4\pi M_s \gamma)^{-1} = 2.63 [\text{ps}]$. Here, our obtained dimensionless coefficient $g_J t_0 / d^3$ can provide the magnitude of the third-order torque which maybe included in some micromagnetic simulations such as OOMMF. In addition, it is noted that the factor of the third-order torque g_J increases linearly with increasing λ_{DW} . However, the exponential decay of $\mathbf{n} \times \partial_y^3 \mathbf{n}$ term will lead to the obtained third-order torque still decreasing with increasing λ_{DW} .

In order to study the movement of Fe DW driven by current, here we consider a one dimension spin chain model, where the local spin of DW is assumed to be uniform in the plane perpendicular to the transport direc-

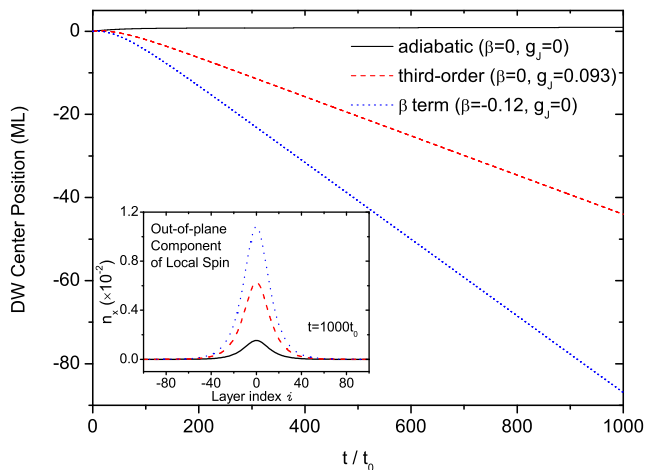


FIG. 8: The time evolution of Fe DW center with $\lambda_{\text{DW}} = 10[\text{ML}]$ at $J = 10^{11}[\text{A/m}^2]$ below the critical current density. Here the unit time is $t_0 = (4\pi M_s \gamma)^{-1}$. One can observe that the velocity driven by the third-order nonadiabatic STT is about half of the wall speed driven by the first-order β term. The inset shows the configuration of out-of-plane component of the local spin at $t = 1000t_0$ for the three cases.

tion. According to the LLG equation and the nonadiabatic STT modeled above, the dynamical equation for the unit vector of local spin in layer i is

$$\begin{aligned} \frac{\partial \mathbf{n}_i}{\partial t} = & -\gamma \mathbf{n}_i \times \mathbf{H}_{\text{eff},i} - \alpha \mathbf{n}_i \times \frac{\partial \mathbf{n}_i}{\partial t} - b_J \frac{\partial \mathbf{n}_i}{\partial y} \\ & - \beta b_J \mathbf{n}_i \times \frac{\partial \mathbf{n}_i}{\partial y} + g_J \mathbf{n}_i \times \frac{\partial^3 \mathbf{n}_i}{\partial y^3} \end{aligned} \quad (6)$$

where the extra β term $-\beta b_J \mathbf{n}_i \times \partial_y \mathbf{n}_i$ is only for comparison. Here i is the site index of one dimension spin chain and the distance between two sites is d , which is unit length used in our dynamical calculations. In the meanwhile, we also use the dimensionless time where the unit time is $t_0 = (4\pi M_s \gamma)^{-1}$. The Gilbert damping coefficient is chosen as $\alpha = 0.02$ and γ is the gyromagnetic ratio. $\mathbf{H}_{\text{eff},i}$ is effective field for the local spin on site i , which is written as⁵¹

$$\mathbf{H}_{\text{eff},i} = H_K n_{z,i} \mathbf{e}_z + 4\pi M_s H_{ex} (\mathbf{n}_{i-1} + \mathbf{n}_{i+1}) - 4\pi M_s n_{x,i} \mathbf{e}_x \quad (7)$$

where H_{ex} is dimensionless exchange constants and H_K is dimensionless anisotropy field. For the equilibrium DW without current, the DW width is determined by $\lambda_{\text{DW}} = \sqrt{H_{ex}/H_K}[\text{ML}]$. Here we take $H_{ex} = 3.0$ and $H_K = 0.03$ so that the width of Fe DW in our simulation is $10[\text{ML}]$. In addition, in our calculations the current density is $J = 10^{11}[\text{A/m}^2]$, so the coefficients in STT terms based on our first-principles calculated results are $b_J = 0.0154$ and $g_J = 0.093$, which are measured in unit time t_0 and unit length d . Further, in order to demonstrate the difference of DW movement between the case of β term and the third-order STT, we also take $\beta = -0.12$, which is chosen

to make the maximum of β term be equal to that of the third-order STT. Hence, given the initial configuration of DW, the above LLG equations for each unit vector of local spin can be solved numerically by Runge-Kutta method.

The position of Fe DW center as function of time with adiabatic and two kinds of nonadiabatic STTs are shown in Fig. 8. As the prediction by the previous studies,^{33,34} our calculated result for the case of only adiabatic STT ($\beta = 0, g_J = 0$) shows that the DW center start to move at first and then will stop inevitably at last. This phenomenon is attributed to the existence of out-of-plane component of local spin,^{52,53} i.e., the local spin will be tilted in x direction after the current have been injected into the DW. As shown in the inset of Fig. 8, one can observe that the out-of-plane component of DW local spin moments in this case will raise up when the DW center stopped. Owing to the shape of DW is film-like, the out-of-plane component of local spin moments can produce the demagnetization field $\mathbf{H}_{\text{demag},i} = -4\pi M_s n_{x,i} \mathbf{e}_x$, which can produce a torque resisting the adiabatic in-plane STT. Therefore, once the demagnetization field increase to be large enough, the velocity of DW center will decrease to zero at last.

The DW movements driven by the nonadiabatic STT of the third- ($\beta = 0, g_J = 0.093$) and first-order ($\beta = -0.12, g_J = 0$) term are also shown in Fig. 8. It can be seen that in both cases the DW will no longer stop and the velocity is nearly constant as the DW center move away from its initial position. The DW velocity induced by the third-order STT is about half of wall speed driven by the β term. From Fig. 8 our obtained wall speed caused by β term is about $5.0[\text{m/s}]$, which is exactly equal to the value of $v = b_J \beta / \alpha$. Note that the DW center move backward in contrast to the case of adiabatic STT. In the inset of Fig. 8, we also show the configuration of the out-of-plane component of local spin at $t = 1000t_0$ for these two cases. Compared with the case of only adiabatic STT, the out-of-plane component of local spin moments with third- and first-order STT are much greater. So the precession around the relative larger demagnetization field will not only resist the adiabatic in-plane STT but also can push the DW moving backward that is in the opposite direction for the case of only adiabatic STT. Moreover, as shown in Fig. 6 the area under the nonadiabatic STT distribution curve for the third-order term is about half as much as that for the β term. Therefore, one can see that the out-of-plane component of local spin at DW center for the third-order STT is also half of the value for the case of β term. As consequence, it will lead to about 50% decrease in the values of both corresponding demagnetization field and velocity for third-order STT compared to the case of β term.

IV. SUMMARY

In summary, we have calculated the current-induced adiabatic and nonadiabatic STTs of Fe, Co and Ni DWs by first-principles noncollinear scattering wave function matching method in the frame of TB-LMTO with ASA approximation. We found that in Co and Ni DWs the spatial distribution of the nonadiabatic STT are in the form of typical nonlocal oscillating torques. However, in contrast to the case of Co and Ni DWs, the out-of-plane component of nonadiabatic STT in Fe DW has localized form. The calculated results also show that the degree of nonadiabaticity in STT of Fe DW is much larger than that of Co and Ni DWs. Further, we found that the distribution of localized nonadiabatic STT in Fe DW can be well fitted by the term of $g_J \mathbf{n} \times \partial_y^3 \mathbf{S}$, which is in the third-order spatial derivative of the local spin instead of the well-known first-order nonadiabatic β term. The coefficient g_J is also obtained for different width λ_{DW} in Fe DW. Finally, the dynamics of local spin in Fe DW driven by the third-order nonadiabatic STT is calculated using

LLG equation. The results show that with the same amplitude of nonadiabatic STT, the velocity of DW center driven by the third-order STT is about half of wall speed caused by the first-order β term.

Acknowledgments

The authors acknowledge Prof. Ke Xia for suggesting the problem and Dr. Shuai Wang for useful discussion about the calculations. The authors are also grateful to Dr. Yuan Xu, Dr. Yong Wang and Dr. Rui Wang for technical assistance. We are grateful to: Ilja Turek for his TB-LMTO-SGF layer code; Anton Starikov for the TB-MTO code based upon sparse matrix techniques. The authors also acknowledge the financial support from the National Natural Science Foundation of China (Grant No:11104247), China Postdoctoral Science Foundation (Grant No:2012M520666), and the Provincial Natural Science Foundation of Zhejiang (Grant No: Y201121807 and Y13A040032).

-
- ¹ M. Hayashi, L. Thomas, Y. B. Bazaliy, C. Rettner, R. Moriya, X. Jiang and S. S. P. Parkin, *Phys. Rev. Lett.* **96** (2006) 197207.
- ² M. Yamanouchi, D. Chiba, F. Matsukura, T. Dietl and H. Ohno, *Phys. Rev. Lett.* **96** (2006) 096601.
- ³ C. Burrowes, A. P. Mihai, D. Ravelosona, J. V. Kim, C. Chappert, L. Vila, A. Marty, Y. Samson, F. Garcia-Sanchez, L. D. Buda-Prejbeanu, I. Tudosa, E. E. Fullerton and J. P. Attane, *Nat. Phys.* **6** (2010) 17.
- ⁴ D. Ilgaz, J. Nievendick, L. Heyne, D. Backes, J. Rhensius, T. A. Moore, M. Á. Niño, A. Locatelli, T. O. Menteş, A. v. Schmidfeld, A. v. Bieren, S. Krzyk, L. J. Heyderman and M. Kläui, *Phys. Rev. Lett.* **105** (2010) 076601.
- ⁵ L. San Emeterio Alvarez, K. Y. Wang, S. Lepadatu, S. Landi, S. J. Bending and C. H. Marrows, *Phys. Rev. Lett.* **104** (2010) 137205.
- ⁶ I. M. Miron, T. Moore, H. Szabolcs, L. D. Buda-Prejbeanu, S. Auffret, B. Rodmacq, S. Pizzini, J. Vogel, M. Bonfim, A. Schuhl and G. Gaudin, *Nat. Mater.* **10** (2011) 419.
- ⁷ A. J. Schellekens, A. van den Brink, J. H. Franken, H. J. M. Swagten and B. Koopmans, *Nat. Commun.* **3** (2012) 847.
- ⁸ T. Koyama, K. Ueda, K.-J. Kim, Y. Yoshimura, D. Chiba, K. Yamada, J.-P. Jamet, A. Mougin, A. Thiaville, S. Mizukami, S. Fukami, N. Ishiwata, Y. Nakatani, H. Kohno, K. Kobayashi and T. Ono, *Nat. Nano.* **7** (2012) 635.
- ⁹ U. Bauer, S. Emori and G. S. D. Beach, *Appl. Phys. Lett.* **101** (2012) 172403.
- ¹⁰ P. Yan, X. S. Wang and X. R. Wang, *Phys. Rev. Lett.* **107** (2011) 177207.
- ¹¹ P. Churemart, R. F. L. Evans and R. W. Chantrell, *Phys. Rev. B* **83** (2011) 184416.
- ¹² A. V. Khvalkovskiy, V. Cros, D. Apalkov, V. Nikitin, M. Krounbi, K. A. Zvezdin, A. Anane, J. Grollier and A. Fert, *Phys. Rev. B* **87** (2013) 020402.
- ¹³ G. Tatara, H. Kohno and J. Shibata, *Physics Reports* **468** (2008) 213.
- ¹⁴ I. Garate, K. Gilmore, M. D. Stiles and A. H. MacDonald, *Phys. Rev. B* **79** (2009) 104416.
- ¹⁵ K. Gilmore, I. Garate, A. H. MacDonald and M. D. Stiles, *Phys. Rev. B* **84** (2011) 224412.
- ¹⁶ T. Taniguchi, J. Sato and H. Imamura, *Phys. Rev. B* **79** (2009) 212410.
- ¹⁷ N. L. Schryer and L. R. Walker, *J. Appl. Phys.* **45** (1974) 5406.
- ¹⁸ J. C. Slonczewski, *J. Magn. Magn. Mater.* **159** (1996) L1.
- ¹⁹ L. Berger, *Phys. Rev. B* **54** (1996) 9353.
- ²⁰ X. R. Wang, P. Yan, J. Lu and C. He, *Ann. Phys. (N. Y.)* **324** (2009) 1815.
- ²¹ X. R. Wang, P. Yan and J. Lu, *Europhys. Lett.* **86** (2009) 67001.
- ²² G. Tatara, *Int. J. Mod. Phys. B* **15** (2001) 321.
- ²³ Y. Hsu and L. Berger, *J. Appl. Phys.* **53** (1982) 7873.
- ²⁴ L. Berger, *J. Appl. Phys.* **55** (1984) 1954.
- ²⁵ P. P. Freitas and L. Berger, *J. Appl. Phys.* **57** (1985) 1266.
- ²⁶ H. Boeve, C. Bruynseraede, J. Das, K. Dessen, G. Borghs, J. De Boeck, R. C. Sousa, L. V. Melo and P. P. Freitas, *IEEE Trans. Magn.* **35** (1999) 2820.
- ²⁷ J. Åkerman, *Science* **308** (2005) 508.
- ²⁸ S. S. P. Parkin, M. Hayashi, and L. Thomas, *Science* **320** (2008) 190.
- ²⁹ L. Thomas, R. Moriya, C. Rettner and S. S. P. Parkin, *Science* **330** (2010) 1810.
- ³⁰ A. Ruotolo, V. Cros, B. Georges, A. Dussaux, J. Grollier, C. Deranlot, R. Guillemet, K. Bouzehouane, S. Fusil and A. Fert, *Nat. Nano.* **4** (2009) 528.
- ³¹ A. Slavin, *Nat. Nano.* **4** (2009) 479.
- ³² Y. B. Bazaliy, B. A. Jones and S.-C. Zhang, *Phys. Rev. B* **57** (1998) R3213.
- ³³ Z. Li and S. Zhang, *Phys. Rev. B* **70** (2004) 024417.
- ³⁴ Z. Li and S. Zhang, *Phys. Rev. Lett.* **92** (2004) 207203.

- ³⁵ S. Zhang and Z. Li, *Phys. Rev. Lett.* **93** (2004) 127204.
- ³⁶ X. Waintal and M. Viret, *Europhys. Lett.* **65** (2004) 427.
- ³⁷ S. E. Barnes and S. Maekawa, *Phys. Rev. Lett.* **95** (2005) 107204.
- ³⁸ J. Xiao, A. Zangwill and M. D. Stiles, *Phys. Rev. B* **73** (2006) 054428.
- ³⁹ A. K. Nguyen, H. J. Skadsem and A. Brataas, *Phys. Rev. Lett.* **98** (2007) 146602.
- ⁴⁰ M. Thorwart and R. Egger, *Phys. Rev. B* **76** (2007) 214418.
- ⁴¹ D. M. Edwards and O. Wessely, *J. Phys.: Condens. Matter* **21** (2009) 146002.
- ⁴² S. Wang, Y. Xu and K. Xia, *Phys. Rev. B* **77** (2008) 184430.
- ⁴³ S. Wang, L. Tang and K. Xia, *Phys. Rev. B* **81** (2010) 094404.
- ⁴⁴ Y. Xu, S. Wang and K. Xia, *Phys. Rev. Lett.* **100** (2008) 226602.
- ⁴⁵ K. Xia, M. Zwierzycki, M. Talanana, P. J. Kelly and G. E. W. Bauer, *Phys. Rev. B* **73** (2006) 064420.
- ⁴⁶ I. Turek *et al.*, *Electronic Structure of Disordered Alloys, Surfaces and Interfaces* (Kluwer, Dordrecht, 1997).
- ⁴⁷ O. K. Andersen and O. Jepsen, *Phys. Rev. Lett.* **53** (1984) 2571.
- ⁴⁸ O. K. Andersen, Z. Pawłowska and O. Jepsen, *Phys. Rev. B* **34** (1986) 5253.
- ⁴⁹ L. Tang and S. Wang, *Mod. Phys. Lett. B* **22** (2008) 2553.
- ⁵⁰ M. D. Stiles and A. Zangwill, *Phys. Rev. B* **66** (2002) 014407.
- ⁵¹ J.-i. Ohe and B. Kramer, *Phys. Rev. Lett.* **96** (2006) 027204.
- ⁵² M. D. Stiles, W. M. Saslow, M. J. Donahue and A. Zangwill, *Phys. Rev. B* **75** (2007) 214423.
- ⁵³ G. Tatara and H. Kohno, *Phys. Rev. Lett.* **92** (2004) 086601.